Biogenesis of Transverse Tubules and Triads: Immunolocalization of the 1,4-Dihydropyridine Receptor, TS28, and the Ryanodine Receptor in Rabbit Skeletal Muscle Developing In Situ

Shaohua Yuan, Wayne Arnold, and Annelise O. Jorgensen

Department of Anatomy, University of Toronto, Toronto, Canada

Abstract. Our previous immunofluorescence studies support the conclusion that the temporal appearance and subcellular distribution of TS28 (a marker of transverse (T) tubules and caveolae in adult skeletal muscle [Jorgensen, A. O., W. Arnold, A. C.-Y. Shen, S. Yuan, M. Gover, and K. P. Campbell. 1990. *J. Cell Biol.* 110:1173–1185]), correspond very closely to those of T-tubules forming de novo in developing rabbit skeletal muscle (Yuan, S., W. Arnold, and A. O. Jorgensen. 1990. *J. Cell Biol.* 110:1187–1198).

To extend our morphological studies of the biogenesis of T-tubules and triads, the temporal appearance and subcellular distribution of the α_1-subunit of the 1,4-dihydropyridine receptor (a marker of the T-tubules and caveolae) was compared to (*a*) that of TS28; and (*b*) that of the ryanodine receptor (a marker of the junctional sarcoplasmic reticulum) in rabbit skeletal muscle cells developing in situ (day 19 of gestation to 10 d newborn) by double immunofluorescence labeling.

The results presented show that the temporal appearance and relative subcellular distribution of the α_1-subunit of the 1,4-dihydropyridine receptor (α_1-DHPR) are distinct from those of TS28 at the onset of the biogenesis of T-tubules. Thus, in a particular developing myotube the α_1-DHPR appeared before TS28 (secondary myotubes; day 19–24 of gestation). Furthermore, the α_1-DHPR was distributed in discrete foci at the outer zone of the cytosol, while TS28 was confined to foci and rod-like structures at the cell periphery. As development proceeded (primary myotubes; day 24 of gestation) ~50% of the foci were positively labeled for both TS28 and the α_1-DHPR, while ~20 and 30% of the foci were uniquely labeled for TS28 and the α_1-DHPR, respectively. The foci labeled for both TS28 and the α_1-DHPR and the foci uniquely labeled for TS28 were generally confined to the cell periphery, while the foci uniquely labeled for the α_1-DHPR were mostly confined to the outer zone of the cytosol. 1–2 d after birth, TS28 was distributed in a chickenwire-like network throughout the cytosol, while the α_1-DHPR was confined to cytosolic foci. In contrast, the temporal appearance and subcellular distribution of the α_1-DHPR and the ryanodine receptor were very similar, if not identical, throughout all the stages of the de novo biogenesis of T-tubules and triads examined.

Assuming that the subcellular distribution of TS28 represents the distribution of forming T-tubules the results presented are consistent with the following plausible scheme for the biogenesis of T-tubules and triads. Before the onset of T-tubule formation, α_1-DHPR–containing cytosolic vesicles form a complex with a ryanodine receptor–containing membrane system (α_1-DHPR: ryanodine receptor-complex). This complex is distributed at the outer zone of the cytosol. After the onset of formation of TS28-containing T-tubules, the α_1-DHPR ryanodine receptor-complex becomes incorporated into discrete regions of the forming T-tubules at the cell periphery. Assuming that α_1-DHPR is complexed with the ryanodine receptor–containing membrane system, incorporation of the α_1-DHPR into T-tubules also results in the formation of a junctional complex between T-tubules and the sarcoplasmic reticulum.

EXCITATION-CONTRACTION coupling in adult skeletal muscle depends on appropriate communication across the narrow gap between transverse (T) tubules and the junctional sarcoplasmic reticulum (SR).[1] This gap is bridged by regularly arranged electron dense structures called "feet" (9). Depolarization of transverse tubules results in Ca^{2+} release from the lumen of the junctional SR, which in

Dr. Yuan's present address is Department of Internal Medicine, University of Nebraska Medical Center, Omaha, NE 68105-7065. Please address reprint requests to the Toronto address.

1. *Abbreviations used in this paper*: DHPR, 1,4-dihydropyridine receptor; SR, sarcoplasmic reticulum.

turn results in contraction. Although the message transmitted from the T-tubules to the junctional SR is still unknown it is generally accepted that the 1,4-dihydropyridine receptor (DHPR) (31) and the ryanodine receptor (6) are essential links in the excitation-contraction coupling.

Biochemical (7) and immunoelectron microscopical studies (16) have demonstrated that the DHPR is densely distributed in the T-tubular membrane. The immunoelectron microscopical studies also showed that the DHPR is present in subsarcolemmal vesicles possibly corresponding to caveolae (16). On the basis of physiological (31) and molecular biological (38, 39) studies it has been proposed that the DHPR functions as a voltage sensor in the excitation–contraction coupling process. Characterization of the highly purified DHPR (4, 5, 10) has shown that it is composed of at least five polypeptide components including the α_1 (155–200 kD), the α_2 (150 kD, reduced), the β (52 kD), the γ (32 kD), and the δ (23–29 kD) subunits. The α_1-DHPR is the DHP binding component of the DHPR.

Immunoelectron microscopical localization of a component of the junctional SR biochemically characterized as the foot protein demonstrated this protein to be localized in the region of the junctional complex between T-tubules and junctional SR in skeletal muscle (18). The ryanodine receptor purified from the junctional SR (12, 13, 25, 37) functions upon reconstitution as the Ca^{2+}-release channel of the SR (12, 25, 37), and its structure (1, 25, 33, 43) corresponds to that of individual foot structures observed in freeze-fracture images of junctional SR (1). Furthermore, the position of every other foot structure corresponds precisely to that of large diamond-shaped clusters of integral membrane particles in the closely apposed junctional T-tubule membrane (1). Assuming that these clusters correspond to DHPRs (26), studies by Block et al. (1) suggested that the DHPR receptor/voltage sensor in the T-tubular membrane may complex with and, thus, activate the ryanodine receptor/Ca^{2+}-release channel of the SR directly.

Despite the functional significance of the T-tubules and the junctional complex between the T-tubules and the junctional SR for excitation–contraction coupling in skeletal muscle, very little is known about the assembly of these structures. Ultrastructural studies have shown that de novo formation of the junctional complex occurs in developing rabbit skeletal muscle between fetal day 22 and 10 d after birth, and is preceded by the onset of the formation of T-tubules which begins at fetal days 17–19 (21).

An ultrastructural study of the formation of T-tubules and SR in developing rat skeletal muscle in situ reported that forming T-tubules first appear as short tubular invaginations of the sarcolemma (19). At the same time, caveolae were frequently encountered at the cell periphery and sometimes observed to be arranged in clusters and short beaded tubular structures. At the onset of their formation T-tubules were mostly present in the subsarcolemmal region and oriented parallel to the longitudinal axis of the myofibers. As development proceeds the T-tubules branch, and extend further towards the interior regions of the myofibers, and their transverse orientation becomes more prominent (19, 34). Before the onset of T-tubular formation SR forms transient junctional complexes with the sarcolemma (19). As T-tubule formation occurs the SR also forms focal junctional complexes with the forming T-tubules. These internal junctional complexes are at first located at the peripheral regions of the cytosol, and only later as the T-tubules extend further toward the central regions of the myofibers are junctional complexes between T-tubules and SR also observed in these regions. Only much later does the transverse orientation of the junctional complexes become prominent and junctional SR continuous along the entire length of the now transversely oriented T-tubules (34). As the formation of interior junctional complexes becomes more extensive the junctional complexes between SR and sarcolemma decrease dramatically (19).

To begin to understand the molecular aspects of the biogenesis of T-tubules we have recently used immunofluorescence labeling techniques to demonstrate that the temporal appearance and subcellular distribution of TS28 (45) (a 28-kD protein marker of T-tubules and caveolae in adult skeletal muscle distinct from the DHPR [17]), correspond very closely to those of T-tubules forming de novo in developing rabbit skeletal muscle (21). These results suggested that TS28 is an excellent marker of T-tubules from the onset of their formation in developing skeletal muscle and support the "add-on" model for the biogenesis of T-tubules first proposed by Schiaffino et al. (35). In accordance with this model we proposed that to initiate the formation of a particular T-tubule a TS28-containing membrane vesicle fuses with the sarcolemma forming a TS28-containing caveolae. However, TS28 in the lipid bilayer of the caveolae is somehow prevented from diffusing into the lateral regions of the sarcolemma. Subsequently, additional TS28-containing vesicles fuse first with the TS28-containing caveola, forming short tubular invaginations in the subsarcolemmal region. Repeated fusions of TS28-containing transfer vesicles with the short TS28-containing tubular structures result in the formation of further extended T-tubules (45).

To further elucidate the sequence of events leading to the de novo biogenesis of functional T-tubules, double immunofluorescence labeling of rabbit skeletal muscle developing in situ was used to compare the temporal appearance and subcellular distribution of the α_1-DHPR to those of TS28 in developing rabbit skeletal muscle during the de novo formation of T-tubules and the junctional complex between T-tubules and junctional SR called triads (day 19 of gestation to 10 d after birth). To begin to understand how the junctional complex between the T-tubules and the junctional SR assembles, the same approach was used to compare the temporal appearance and subcellular distribution of TS28 and the α_1-DHPR to those of the ryanodine receptor, a marker of the junctional region of the SR.

The results of these studies are consistent with the idea that before the onset of T-tubule formation, α_1-DHPRs form complexes with ryanodine receptors which accumulate in the outer zone of the cytosol. After the onset of formation of TS28-containing T-tubules, the α_1-DHPR ryanodine receptor complexes become incorporated into forming T-tubules, thus, possibly simultaneously incorporating the DHPR into discrete regions of the T-tubular membrane and forming a junctional complex between T-tubules and the SR.

Materials and Methods

Preparation of Tissue Extract, Membrane Fractions, and Purification of Proteins from Rabbit Skeletal Muscle

Skeletal muscle extracts represent the supernatant obtained by extracting

quick-frozen tissue with an SDS-containing buffer as outlined below. Muscle tissue was quickly dissected, frozen in liquid N_2, and powdered with a precooled mortar and pestle. The muscle powder was extracted for 5 min at room temperature with buffer A (10% SDS, 10 mM EDTA, 0.1 M Tris, 50 mM DTT, and 0.1 mM PMSF, pH 8.0) at a ratio of 100 mg/ml (net weight/vol). The extracts were centrifuged for 15 min at 12,800 *g* (Eppendorf centrifuge 5412; Brinkmann Instruments Co., Westbury, NY) and the supernatant was used immediately for SDS-PAGE. The DHPR was purified as described by Campbell and Kahl (3). The ryanodine receptor was purified as described by Imagawa et al. (12). Protein concentrations were determined by the method of Lowry et al. (27) as modified by Peterson (29) using BSA as a standard.

Preparations and Characterization of Monoclonal and Polyclonal Antibodies

TS28. $IXE11_2$ to TS28 was prepared and characterized as previously described (17).

α_1-DHPR. Polyclonal antibodies to purified DHPR were raised in guinea pigs by a series of intraperitoneal injections as described by Tung (41). The presence and specificity of antibodies to the α_1-DHPR were determined by immunoblotting of SDS-PAGE-separated skeletal muscle extract, purified DHPR, and ryanodine receptor. Affinity-purified antibodies to the α_1-DHPR from rabbit skeletal muscle were prepared from guinea pig ascites according to the methods of Fowler and Bennet (8) using a DHPR-nitrocellulose paper complex (100 μg DHPR/square inch nitrocellulose paper) as the affinity column.

Ryanodine Receptor. Polyclonal antibodies to immunoaffinity-purified ryanodine receptor from rabbit skeletal muscle (12) were produced in sheep as previously described (23). Briefly, antiserum was raised in a sheep by a series of intramuscular injections with 0.5 mg of purified ryanodine receptor. The presence and specificity of antibodies to the rabbit skeletal ryanodine receptor was determined by immunoblotting of SDS-PAGE-separated, purified ryanodine receptor, DHPR, and skeletal muscle extracts.

Affinity-purified antibodies to the rabbit skeletal ryanodine receptor were prepared from sheep antiserum according to the procedure of Fowler and Bennett (8) using a purified ryanodine receptor-nitrocellulose paper complex (100 μg ryanodine receptor/square inch nitrocellulose paper) as the affinity column.

Immunoblotting

SDS-PAGE was performed by the method of Laemmli (24) using either a 7.5% continuous polyacrylamide separating gel or a discontinuous separating gel where the top and bottom half of the separating polyacrylamide gel was 3.0 and 7.5%, respectively. Transelectrophoresis of SDS-PAGE separated proteins onto nitrocellulose and subsequent immunoblotting was performed according to the methods of Towbin et al. (40) with minor modification as outlined below.

Nitrocellulose blots were blocked in 5% nonfat dry milk in TBS (20 mM TRIS, 500 mM NaCl, pH 7.4) (14). The antibody incubation medium included 2.5% nonfat dry milk in TTBS (TBS containing 0.05% Tween 20). For immunoblotting of the DHPR, the blots were incubated for 1 h with guinea pig antibodies to the α_1-DHPR (1:1,000 dilution). The blots were then washed to remove unbound antibody, incubated with affinity-purified goat anti-guinea pig IgG conjugated to alkaline phosphatase (1:3,000 dilution; Biorad Laboratories, Ltd., Richmond, CA) in 2.5% nonfat dry milk in TTBS. The blots were rinsed twice with TTBS for 5 min each and TBS for 10 min. Color development was completed using 5-Bromo-4-chloro-3-indolyl phosphate-toluidine salt (BCIP)/p-nitro blue tetrazolium chloride (NBT) substrate reagents (BCIP/NBT; Biorad Laboratories Ltd.). All procedures were performed at room temperature with gentle agitation. The reaction was terminated by thoroughly rinsing the blots with water and allowing them to air dry. Immunoblotting with sheep antibodies to the ryanodine receptor was carried out as described above except that a triple-layered procedure was used. Thus, the incubation with sheep antibodies to the ryanodine receptor (1/500 dilution) was followed first by an incubation with affinity-purified goat anti-sheep IgG conjugated to biotin (1:1,000 dilution; Biorad Laboratories Ltd.) and then by an incubation with avidin-conjugated alkaline phosphatase (1:1,000 dilution; Biorad Laboratories Ltd.).

Dissection, Fixation, and Cryosectioning

Hind limb muscle tissues were dissected from rabbits at different stages of development ranging from day 19 of gestation to 2 d after birth. Bundles of myofibers from 10-d and adult rabbit gracilis muscle were dissected and tied to tooth picks at 100–120% of rest length, fixed in 2% paraformaldehyde, and infused with 0.6 M sucrose as previously described (15). Small blocks of fixed and unfixed muscle tissues were cryofixed in isopentane, precooled in liquid N_2. Cryostat sections (6–8 μm) were cut, fixed in 70% ethanol at 0°C for 5 min, air dried, and stored in a desiccator at −20°C until use.

Indirect Immunofluorescence Labeling

Single Immunofluorescence Labeling. Immunofluorescence labeling of 6–8-μm cryosections of fixed and unfixed muscle tissues was carried out as previously described (15). Briefly, the sections were first labeled with one of the following antibodies: (*a*) affinity-purified guinea pig antibodies to the α_1-DHPR (10 μg/ml); (*b*) mAb $IXE11_2$ to TS28 (1.74 μg/ml); and (*c*) affinity-purified sheep antibodies to the ryanodine receptor (10 μg/ml). The corresponding secondary antibodies were (*a*) $F(ab')_2$ fragments of rabbit anti-guinea pig IgG conjugated to FITC (1:40 dilution; Organon Teknika Co., West Chester, PA); (*b*) $F(ab')_2$ fragments of affinity-purified rabbit anti-mouse IgG conjugated to rhodamine (1:80 dilution; Jackson Immunoresearch Laboratories Inc., West Grove, PA); and (*c*) $F(ab')_2$ fragments of affinity-purified rabbit anti-sheep IgG conjugated to fluorescein or rhodamine (1:40 dilution; Jackson Immunoresearch Laboratories Inc.).

Controls. For adsorption, 10 μg/ml of affinity-purified antibodies to the DHPR was incubated with 0 and 60 μg/ml purified DHPR as previously described (15). Similarly, 10 μg/ml of affinity-purified antibodies to the ryanodine receptor was incubated with 0 and 60 μg/ml purified ryanodine receptor. The molar ratio of antigen/antibody is ~2 for the adsorption of both antibodies. The supernatants obtained by centrifugation were used as the primary reagent in the single indirect immunolabeling assay.

Double Immunofluorescence Labeling. Double immunofluorescence labeling of 6–8-μm cryosections was carried out in sequential steps combining two of the three single immunofluorescence labeling procedures described above. Double-labeling procedure A was composed of single-labeling procedure a for the α_1-DHPR followed by labeling procedure b for TS28. Double labeling procedure B was composed of single labeling procedure a for the α_1-DHPR followed by procedure c for the ryanodine receptor where a rhodamine-conjugated secondary antibody was used to label the ryanodine receptor. Double-labeling procedure C was composed of single-labeling procedure c for the ryanodine receptor followed by labeling procedure b for TS28. In procedure C, a fluorescein-conjugated secondary antibody was used to label the ryanodine receptor.

Conventional fluorescence microscopy was carried out with a Zeiss photomicroscope provided with an epifluorescence attachment and a phase-contrast condenser. Confocal fluorescence microscopy was carried out with a Nikon photomicroscope provided with a Lasersharp MRC-500 confocal fluorescence imaging system, using a dual channel detection system and an

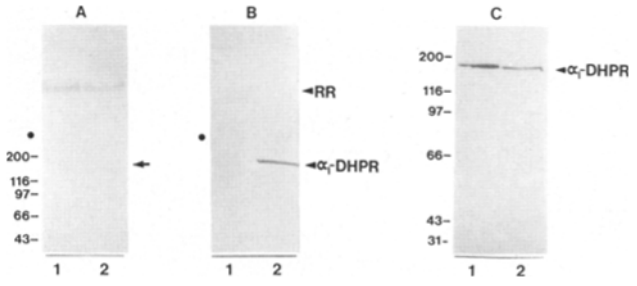

Figure 1. Characterization of antibodies to the DHPR and the ryanodine receptor by immunoblotting. Rabbit muscle extracts (*A–C*, lane *2*; 5 μl)/purified DHPR (*C*, lane *1*; 0.1 μg) and purified ryanodine receptor (*A* and *B*, lane *1*; 4 μg) were prepared, separated by SDS-PAGE followed by immunoblotting with sheep antiserum to the ryanodine receptor (*A*) and guinea pig antibodies to the DHPR (*B* and *C*) as described in Materials and Methods. SDS-PAGE of the lanes shown in *A* and *B* were performed using 3%/7.5% discontinuous polyacrylamide as the separating gel. (The filled circle in *A* and *B* indicate the border between the upper 3% and the lower 7.5% polyacrylamide gel.) SDS-PAGE of the lanes in *C* was performed using continuous 7.5% polyacrylamide as the separating gel.

Argon laser for illumination (Biorad Laboratories Canada Ltd., Mississauga, Canada) (44). The distribution of FITC-conjugated secondary antibodies was visualized by illumination with a laser line at 488 nm. The distribution of rhodamine-conjugated secondary antibodies was visualized by illumination with a laser line at 515 nm. The photographs were taken from an attached photo-recording system with high linearity.

Analysis of the Relative Distribution of α_1-DHPR and TS28 in 24-d Fetal Skeletal Muscle

Paired confocal images showing the relative spatial distribution of α_1-DHPR (see Fig. 4, *c*) and TS28 (see Fig. 4 *d*) in primary myofibers (n = 15) present in transverse cryosections of 24-d fetal skeletal muscle double labeled for these two proteins were traced (see Fig. 4, *e* and *f*) in two different colors (not shown) and superimposed. By superimposing the paired tracings, three distinct classes of fluorescently labeled foci were identified as illustrated in Fig. 4 *j*. One class of foci were labeled for both α_1-DHPR and TS28 (see Fig. 4 *j*, *crosses*), another class of foci was uniquely labeled for α_1-DHPR (see Fig. 4 *j*, *open circles*), while a third class was uniquely labeled for TS28 (see Fig. 4 *j*, *open triangles*). The sum of the number of foci in each of the three classes represents the total number of labeled foci in a particular cell. Next, the total foci and the foci in each of the three classes of foci were enumerated for each of the cells analyzed. Subsequently, the percentage of labeled foci in each of the three classes was calculated for each cell. Finally, the percentage of foci in each class was averaged over the number of cells analyzed and an SD calculated.

Results

Characterization of Antibodies to the DHPR and the Ryanodine Receptor

The specificity of the sheep antiserum towards the ryanodine receptor purified from rabbit skeletal muscle triads was demonstrated by immunoblotting of SDS-PAGE-separated ryanodine receptor and tissue extract from rabbit skeletal muscle (Fig. 1 *A*). The sheep antiserum bound to a single band present in the muscle extract (Fig. 1 *A*, lane *2*). The electrophoretic mobility of this band corresponds to that of the ryanodine receptor purified from rabbit skeletal muscle (Fig. 1 *A*, lane *1*). Furthermore, the sheep antiserum to the ryanodine receptor did not bind to the α_1-DHPR also present in the muscle extract (Fig. 1 A, lane 2, *arrow*) as demonstrated by immunoblotting of the same extract with antibodies to the α_1-DHPR (Fig. 1 *B*, lane *2*).

Similarly, the specificity of the ascites from guinea pigs immunized with purified DHPR towards the α_1-DHPR was demonstrated by immunoblotting of SDS-PAGE-separated DHPR (Fig. 1 *C*, lane *1*), tissue extracts (Fig. 1 *B*, lane *2* and Fig. 1 *C*, lane *2*), and ryanodine receptor from rabbit skeletal muscle (Fig. 1 *B*, lane *1*). The guinea pig antibodies to the DHPR bound to a single band with an apparent M_r of 170,000 D present in the muscle extract (Fig. 1 *B*, lane *2* and 1 *C*, lane *2*). The electrophoretic mobility of the 170,000-D band in the muscle extract (Fig. 1 *C*, lane *2*) corresponds to that of the α_1-DHPR of the DHPR purified from rabbit skeletal muscle (Fig. 1 *C*, lane *1*). However, the guinea pig antibodies did not bind to either the purified ryanodine receptor (Fig. 1 *B*, lane *1*) or to the ryanodine receptor present in the muscle extract (Fig. 1 *B*, lane *2*), as demonstrated by immunoblotting of the same extract with sheep antibodies to the ryanodine receptor (Fig. 1 *A*, lane *2*).

These results show that the guinea pig antibodies to the DHPR specifically bind to the α_1-DHPR of the DHPR and that they do not cross react with the ryanodine receptor. They also show that the sheep antiserum to the ryanodine receptor is specific for the ryanodine receptor and does not cross react with the α_1-DHPR.

Subcellular Distribution of the α_1-DHPR, the Ryanodine Receptor, and TS28 in Skeletal Muscle Developing In Situ

To determine the temporal appearance and subcellular distribution of the DHPR in relation to that of TS28, the subcellular distribution of the α_1-DHPR was compared to that of TS28 in skeletal muscle developing in situ by double immunofluorescence labeling (day 19 of gestation to 15 d after birth). To determine temporal appearance and the subcellular distribution of the junctional complex between the T-tubules and the junctional SR assumed to represent the forming triad, the temporal appearance and subcellular distribution of the α_1-DHPR and of TS28 were also compared to that of the ryanodine receptor by double immunofluorescence labeling of cryosections from rabbit skeletal muscle developing in situ.

Fetal Day 19–24

A mixture of myofibers with large and small diameters was observed in transverse sections at this stage of development. We assume that the large and small myofibers correspond to "primary" and "secondary" myotubes, respectively, as previously described in developing rat (20) and chick (28) skeletal muscle. Since the developmental stage of primary myotubes is ahead of that of the surrounding "secondary" myotubes, a mixture of myofibers at various stages of development is present in sections from rabbit hind limbs between fetal day 19 and day 24 of gestation.

α_1-DHPR versus TS28. Examination of transverse cryosections from 19–24-d-old fetal rabbit skeletal muscle following double labeling for the α_1-DHPR (Fig. 2, *a* and *c*) and for TS28 (Fig. 2, *b* and *d*) showed that labeling for the α_1-DHPR was present in all large primary (Fig. 2 *a*, *arrows*) and all small secondary myotubes (Fig. 2 *a*, *single and double arrowheads*), while that for TS28 was present in all primary myotubes (Fig. 2 *b*, *arrows*) and some (Fig. 2 *b*, *single arrowhead*) but not all small secondary myotubes (Fig. 2 *b*, *double arrowheads*). The labeling for the α_1-DHPR was distributed in discrete foci present at both the cell periphery and the interior regions of both primary (Fig. 2, *a* and *c*, *arrows*) and secondary myotubes (Fig. 2, *a* and *c*, *single and double arrowheads*). In contrast, TS28 as previously shown (45) was mostly confined to foci and rod-like structures at the cell periphery of the corresponding primary myotubes (Fig. 2, *b* and *d*, *arrows*), and some (Fig. 2, *b* and *d*, *single arrowheads*) but not all secondary myotubes (Fig. 2 *b*, *double arrowheads*). However, at this stage of development foci and rod-like structures positively labeled for TS28 were also present in the outer regions of the cytosol of some primary myofibers (Fig. 2 *d*, *arrow*). The results presented suggest that the first appearance of the α_1-DHPR in secondary myotube precedes that of TS28. Furthermore, it is particularly obvious that the distribution of a considerable proportion of foci at the cell periphery of myotubes positively labeled for the α_1-DHPR (Fig. 2, *a* and *c*, *single arrowheads*) is distinct from that of the foci and rod-like structures at the periphery of the corresponding myotubes positively labeled for TS28 (Fig. 2, *b* and *d*, *single arrowheads*). The

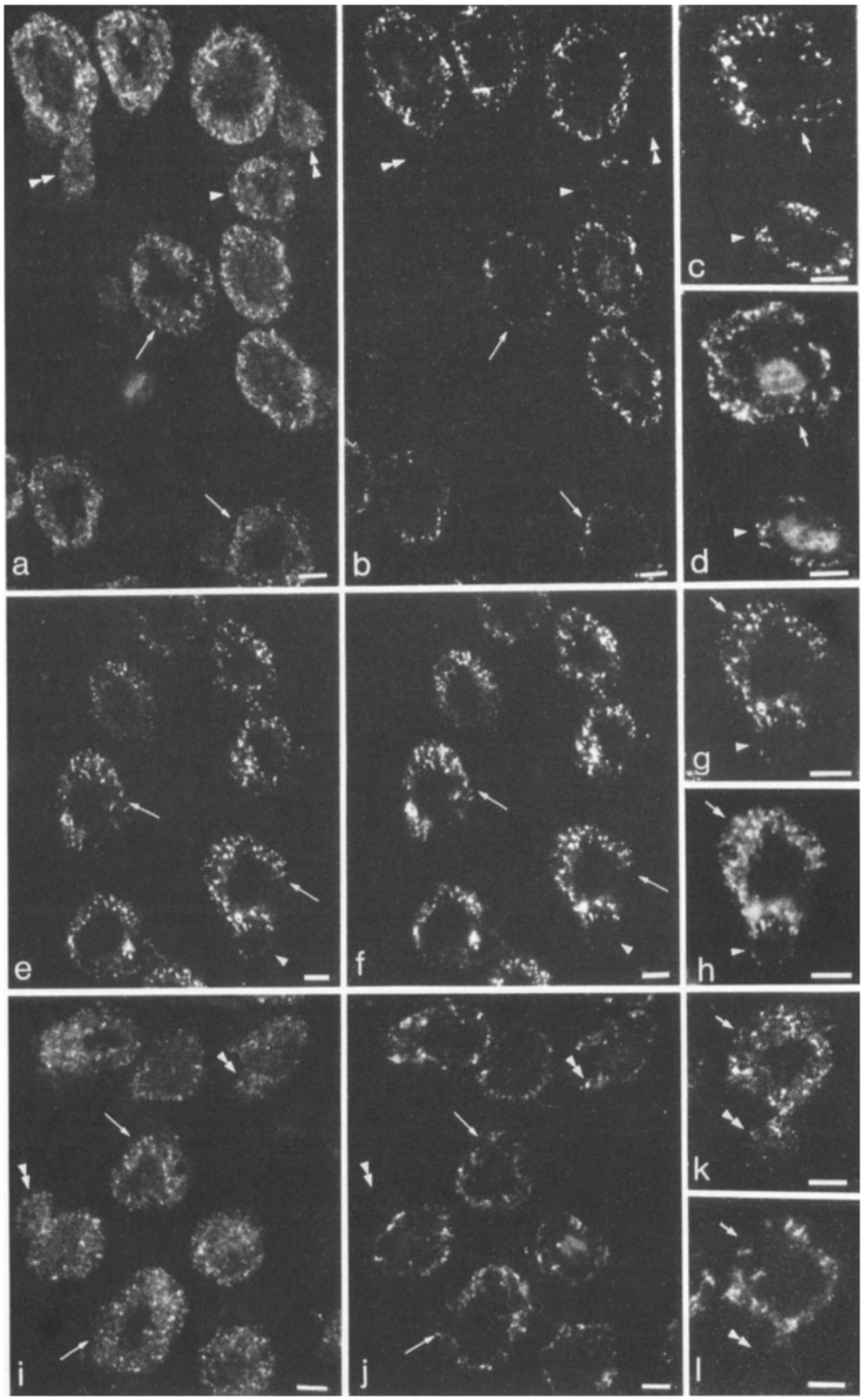

Figure 2. Localization of the α_1-DHPR, the ryanodine receptor, and TS28 in transverse cryosections of unfixed 19–24-d-old fetal rabbit skeletal muscle by conventional immunofluorescence microscopy. Transverse sections were double immunolabeled with (*1*) affinity-purified antibodies to the α_1-DHPR (*a* and *c*) and with mAb IXE11$_2$ to TS28 (*b* and *d*) (procedure A); (*2*) affinity-purified antibodies to the α_1-DHPR (*e* and *g*) and with affinity-purified antibodies to the ryanodine receptor (*f* and *h*) (procedure B); and (*3*) affinity-purified antibodies to the ryanodine receptor (*i* and *k*) and with mAb IXE11$_2$ to TS28 (*j* and *l*) (procedure C). Specific labeling for TS28 is present in all primary myotubes (*b* and *j*, *arrows*) and some (*b*, *single arrowhead*) but not all secondary myotubes (*b* and *j*, *double arrowheads*). TS28 labeling in primary and some secondary myotubes is confined to discrete foci or rod-like structures at the cell periphery (*b*, *d*, *j*, and *l*; *arrows* and *single arrowheads*). These rod-like structures extend from the cell periphery towards the center of the cell in some myotubes (*d*, *arrowhead* and *l*; *arrows*). In contrast, specific labeling for both the α_1-DHPR (*a*, *c*, *e* and *g*) and the ryanodine receptor (*f*, *h*, *i*, and *k*) is present in discrete foci in the outer zone of the cytosol in both primary and secondary myotubes (*a* and *e*, *f* and *i*; *arrows*, *single* and *double arrowheads*). It is noteworthy that most of the foci labeled for the α_1-DHPR (*e* and *g*) are also labeled for the ryanodine receptor (*f* and *h*). Bars, 5 μm.

possibility that lack of TS28 labeling of α_1-DHPR-positive foci is due to steric hindrance is highly unlikely since the same results were obtained when labeling for TS28 preceded that for α_1-DHPR in the double immunofluorescence labeling experiments.

Examination of longitudinal cryosections from 19–24-d-old fetal rabbit skeletal muscle following double labeling for the α_1-DHPR (Fig. 3 *a*) and for TS28 (Fig. 3 *b*) confirmed the results obtained by double labeling of transverse sections (Fig. 2, *a–d*). Thus, labeling for the α_1-DHPR was localized

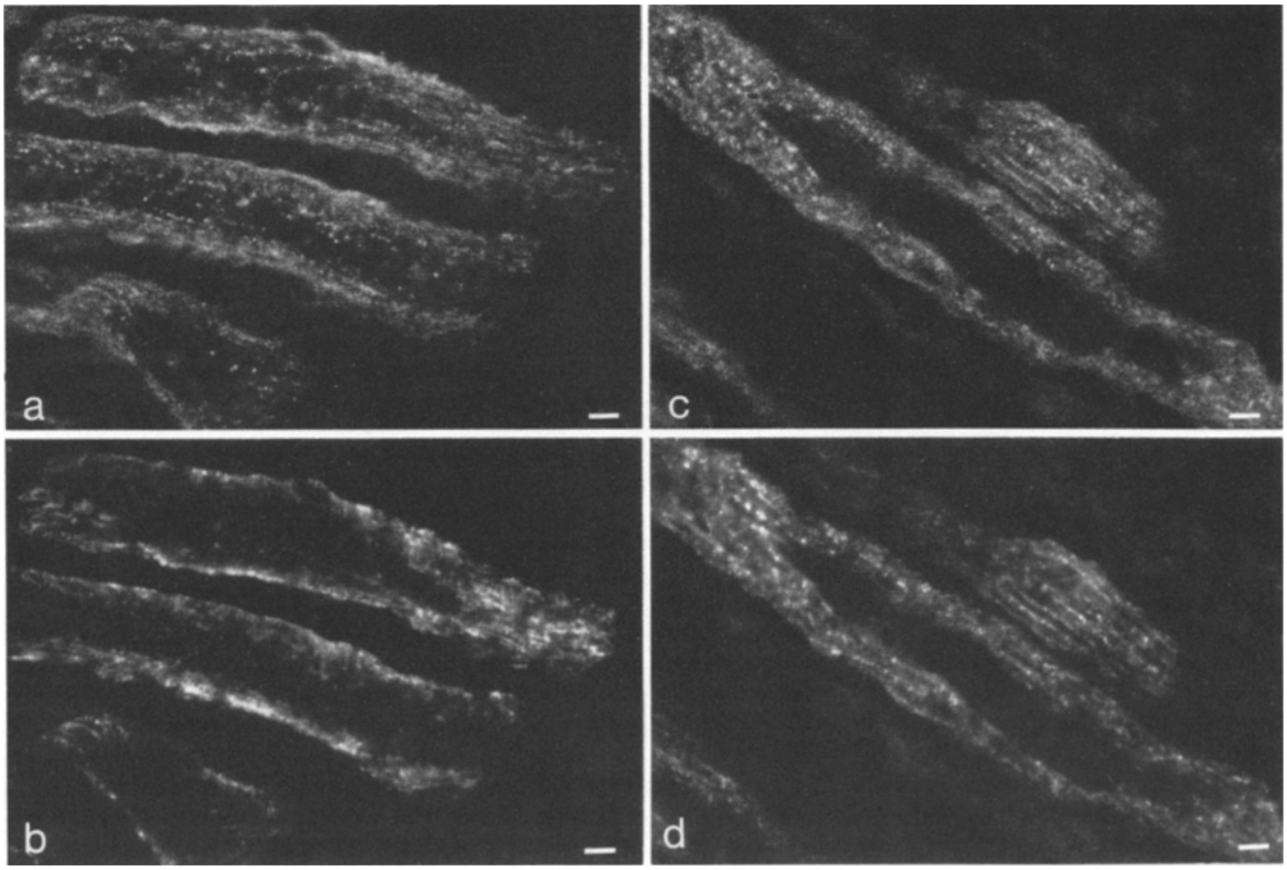

Figure 3. Localization of the α_1-DHPR, the ryanodine receptor, and TS28 in longitudinal cryosections of unfixed 19–24-d-old fetal rabbit skeletal muscle by conventional immunofluorescence microscopy. A longitudinal section was double immunolabeled (procedure A) with affinity-purified antibodies to the α_1-DHPR (*a*) and mAb IXE11$_2$ to TS28 (*b*) by the indirect immunofluorescence labeling technique (see Materials and Methods). Similarly, a longitudinal section was double immunolabeled (procedure B) with affinity-purified antibodies to the α_1-DHPR (*c*) and the ryanodine receptor (*d*). Specific labeling for the α_1-DHPR is present as discrete foci in the outer zone of the cytosol (*a* and *c*). Most of the foci immunolabeled for the α_1-DHPR (*c*) are also labeled for the ryanodine receptor (*d*). In contrast, specific labeling of TS28 is mostly present at the cell periphery (*b*). Bars, 5 μm.

to discrete foci present at both the cell periphery and the outer zone of the cytosol (Fig. 3 *a*), while the labeling for TS28 was mostly confined to the cell periphery (Fig. 3 *b*). These results imply that the α_1-DHPR and TS28 may in part colocalize at the cell periphery and that the α_1-DHPR is present in discrete foci in the central region of the developing myotube where TS28-containing T-tubules are not yet present.

α_1-DHPR versus Ryanodine Receptor. Examination of transverse sections double labeled for the α_1-DHPR (Fig. 2, *e* and *g*) and for the ryanodine receptor (Fig. 2, *f* and *h*) showed that specific labeling for both proteins was present in discrete foci in the outer zone of the cytosol of both primary (Fig. 2, *e* and *f*, *arrows*) and secondary myotubes (Fig. 2, *e* and *f*, *arrowheads*). Furthermore, it was observed that a majority of the foci labeled for the α_1-DHPR in both primary (Fig. 2, *e* and *g*, *arrows*) and secondary myotubes (Fig. 2, *e* and *g*, *arrowheads*) was also labeled for the ryanodine receptor (Fig. 2, *f* and *h*; *arrows* and *arrowheads*, respectively).

Examination of longitudinal cryosection from 19–24-d fetal rabbit skeletal muscle following double labeling for the α_1-DHPR (Fig. 3 *c*) and for the ryanodine receptor (Fig. 3 *d*) confirmed the results obtained by double labeling of transverse sections (Fig. 2, *e–h*). Thus, the distribution of labeling for the α_1-DHPR present in discrete foci in the cytosol (Fig. 3 *c*) corresponded very closely to that of the ryanodine receptor (Fig. 3 *d*).

Ryanodine Receptor versus TS28. Examination of transverse sections double labeled for the ryanodine receptor (Fig. 2, *i* and *k*) and for TS28 (Fig. 2, *j* and *l*) showed that positive labeling for the ryanodine receptor was present in all primary (Fig. 2, *i* and *k*, *arrows*) and secondary myotubes (Fig. 2, *i* and *k*, *double arrowheads*), while that for TS28 was present in all primary myotubes (Fig. 2, *j* and *l*, *arrows*) and some (not shown) but not all secondary myotubes (Fig. 2, *j* and *l*, *double arrowheads*). These results indicate that the first appearance of the ryanodine receptor in a particular secondary myotube precedes that of TS28. As expected on the basis of the results presented above (Fig. 2, *b*, *d*, *f*, and *h*), specific labeling for the ryanodine receptor in primary myotubes was present in discrete foci in the outer zone of the cytosol (Fig. 2, *i* and *k*), while specific labeling for TS28 was mostly confined to discrete foci and rod-like structures at the cell periphery (Fig. 2, *j* and *l*).

Confocal Imaging of α_1-DHPR versus TS28. To com-

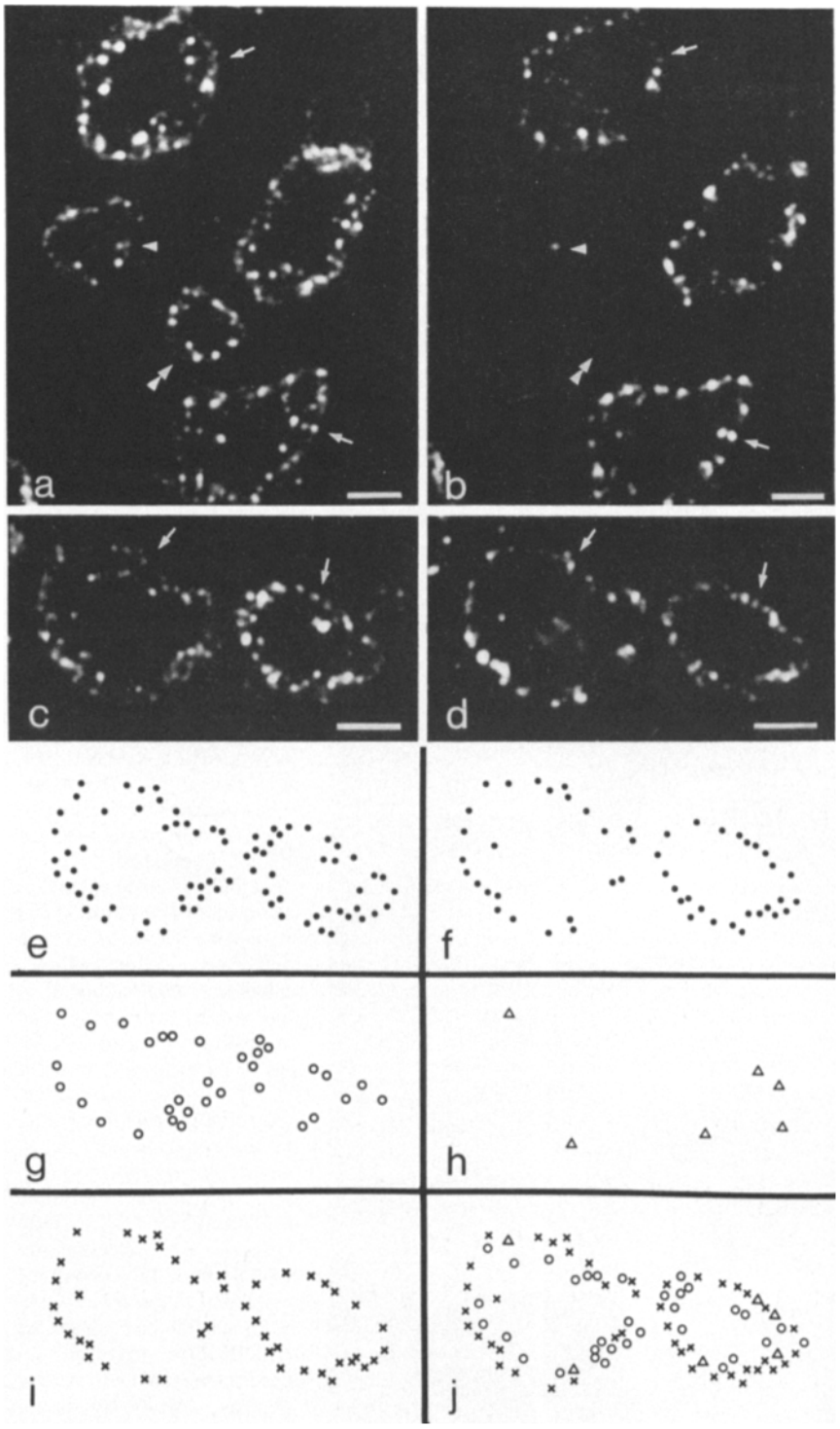

Figure 4. Localization of the α_1-DHPR and TS28 in transverse sections from 24-d-old fetal skeletal muscle by confocal microscopy. A 6–8-μm transverse cryosection of unfixed 24-d-old fetal skeletal muscle was double immunolabeled (procedure A) with affinity-purified antibodies to the α_1-DHPR (*a* and *c*) and with mAb $IXE11_2$ to TS28 (*b* and *d*), and examined by confocal microscopy (0.2-μm optical section). Specific labeling for both the α_1-DHPR (*a* and *c*) and for TS28 (*b* and *d*) is present in discrete foci. The foci positively labeled for the α_1-DHPR are distributed at the cell periphery and outer zone of the cytosol of primary (*a* and *c*, *arrows*) and secondary myotubes (*a*, *single* and *double arrowheads*). In contrast, foci strongly labeled for TS28 are almost exclusively distributed at the cell periphery of primary myotubes (*b* and *d*, *arrows*). Occasionally, faintly labeled foci are observed at the cell periphery of some secondary myotubes (*b*, *single arrowhead*). Other secondary myotubes positively labeled for the α_1-subunit (*a*, *double arrowhead*) are not labeled for TS28 (*b*, *double arrowhead*). Tracings of the subcellular distribution of foci in the two primary myotubes positively labeled for the α_1-DHPR (*c*) TS28 (*d*) are shown in *e* and *f* (*black dots*), respectively. Superimposing the tracings shown in *e* and *f* identifies three classes of foci: (*1*) foci uniquely labeled for α_1-DHPR (*g* and *j* [*open circles*]); (*2*) foci uniquely labeled for TS28 (*h* and *j* [open triangles]); and (*3*) foci labeled for both α_1-DHPR and TS28 (*i* and *j*, *crosses*). Comparison between the spatial distribution of these three classes of foci as presented in *j* shows that foci uniquely labeled for α_1-DHPR are usually present in the outer zone of the cytosol (*j*, *open circles*), while foci uniquely labeled for TS28 are mostly present at the cell periphery (*j*, *open triangles*). The foci labeled for both the α_1-subunit and the TS28 are also mainly distributed in the cell periphery (*j*, *crosses*). Bars, 5 μm.

pare in more detail the distribution of the α_1-DHPR (Fig. 2, *a* and *c*) and TS28 (Fig. 2, *b* and *d*) at the early stages of formation of T-tubules (19–24 day of gestation), transverse sections double labeled for both proteins were examined by confocal microscopy which provides a Z-axis resolution of ~0.8 μm (2). Fig. 4 shows confocal images of thin optical sections from the central region of a 6–8-μm transverse cryosection of 24-d-old fetal skeletal muscle double labeled for the α_1-DHPR (Fig. 4, *a* and *c*) and for TS28 (Fig. 4, *b* and *d*). Generally, the images obtained in confocal microscopy were similar to those obtained by conventional immunofluorescence microscopy. Thus, it was observed that positive labeling for both the α_1-DHPR (Fig. 4, *a* and *c*) and for TS28 (Fig. 4, *b* and *d*) was distributed in discrete foci of all primary (Fig. 4, *a–d*, *arrows*) and secondary myotubes (Fig. 4, *a* and *b*; *single arrowhead*). Other secondary myotubes were also labeled for the α_1-DHPR (Fig. 4 *a*, *double arrowhead*), but not for TS28 (Fig. 4 *b*, *double arrowhead*). It is noteworthy, however, that a much higher proportion of the foci positively labeled for TS28 was confined to the cell

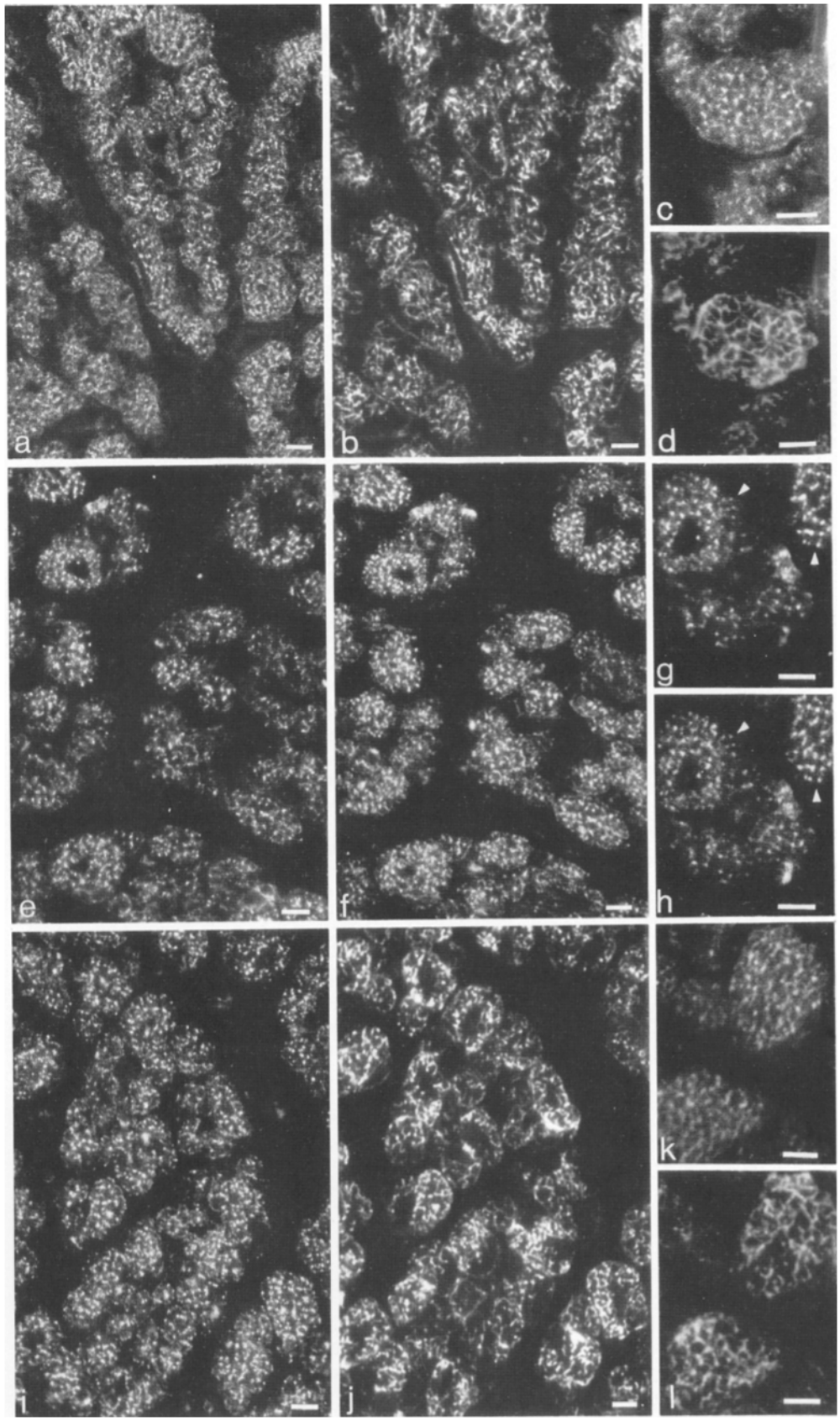

Figure 5. Localization of the α_1-DHPR, the ryanodine receptor, and TS28 in transverse cryosections of unfixed 1–2 d newborn rabbit skeletal muscle by conventional immunofluorescence microscopy. Transverse sections were double immunolabeled with (*1*) affinity-purified antibodies to the α_1-DHPR (*a* and *c*) and with mAb IXE11$_2$ to TS28 (*b* and *d*) (procedure A); (*2*) affinity-purified antibodies to the α_1-DHPR (*e* and *g*) and with affinity-purified antibodies to the ryanodine receptor (*f* and *h*) (procedure B); and (*3*) affinity-purified antibodies to the ryanodine receptor (*i* and *k*) and with mAb IXE11$_2$ to TS28 (*j* and *l*) (procedure C). Specific labeling for TS28 is distributed in a chickenwire-like network throughout the cytosol (*b*, *d*, *j*, and *l*). In contrast, specific labeling for the α_1-DHPR (*a*, *c*, *e*, and *g*) and for the ryanodine receptor (*f*, *h*, *i*, and *k*) are mostly confined to discrete foci present throughout the cytosol. The subcellular distribution of foci labeled for the α_1-DHPR (*e* and *g*, *arrowhead*) corresponds very closely to that of the foci labeled for the ryanodine receptor (*f* and *h*, *arrowhead*). Bars, 5 μm.

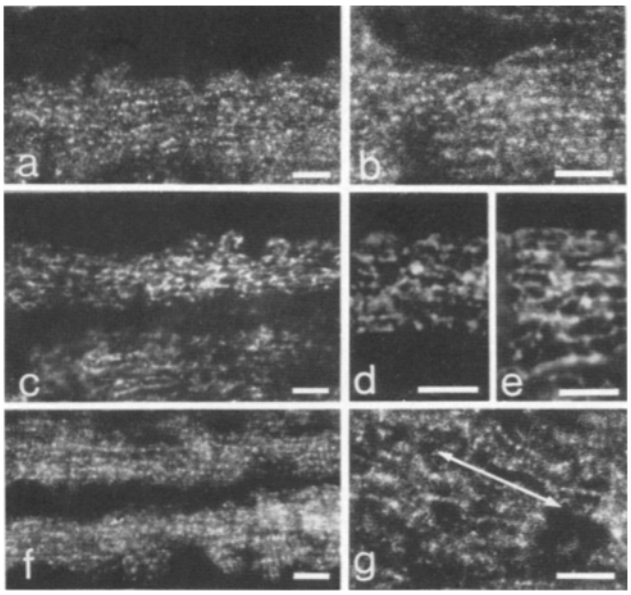

Figure 6. Localization of the α_1-DHPR, the ryanodine receptor, and TS28 in longitudinal cryosections of unfixed 1–2-d newborn rabbit skeletal muscle by conventional immunofluorescence microscopy. Longitudinal sections were immunolabeled with affinity-purified antibodies to the α_1-DHPR (*a* and *b*), with mAb $IXE11_2$ to TS28 (*c*, *d*, and *e*), and with affinity-purified antibodies to the ryanodine receptor (*f* and *g*, *arrow* indicates approximate longitudinal orientation of myotube). Specific labeling for TS28 is distributed in an anastomosing network composed of both longitudinally and transversely oriented fiber-like structures (*c*, *d*, and *e*). In contrast, specific labeling for either the α_1-DHPR (*a* and *b*) or the ryanodine receptor (*f* and *g*) is present in discrete foci throughout the cytoplasm of the myofibers. Bars, 5 μm.

periphery when transverse sections were imaged by confocal microscopy (Fig. 4, *b* and *d*) than when imaged by conventional epifluorescence microscopy (Fig. 2, *b*, *d*, *j*, and *l*). This is probably to some extent due to the fact that imaging of slightly oblique 6–8-μm transverse sections of small myotubes by conventional microscopy could make it appear as if some of the peripherally located foci were present in the outer regions of the cytosol.

To determine more precisely the spatial distribution of the fluorescent foci positively labeled for α_1-DHPR (Fig. 4 *c*) and TS28 (Fig. 4 *d*) in 24-d fetal primary myotubes, tracings of the foci labeled for α_1-DHPR (Fig. 4 *e*) and TS28 (Fig. 4 *f*) were superimposed (Fig. 4 *j*). Examination of the superimposed tracings (Fig. 4 *j*) revealed three classes of foci, namely (*a*) foci uniquely labeled for α_1-DHPR (Fig. 4, *g* and *j*, *open circles*); (*b*) foci uniquely labeled for TS28 (Fig. 4, *h* and *j*, *open triangles*); and (*c*) foci labeled for both α_1-DHPR and TS28 (Fig. 4, *i* and *j*, *crosses*). Analysis of superimposed tracings of the distribution of fluorescent foci in primary myotubes (n = 15) present in transverse sections of 24-d fetal muscle double labeled for the α_1-DHPR and for TS28 by confocal microscopy showed that 47 $\pm$ 15% of the foci were labeled for both the α_1-DHPR and TS28, while 21 $\pm$ 10% and 31 $\pm$ 12% of the foci were uniquely labeled for TS28 and the α_1-DHPR, respectively. Furthermore, qualitative examination of the spatial distribution of the three classes of foci showed that many of the foci uniquely labeled for the α_1-DHPR were distributed in the outer zone of the cytosol (Fig. 4 *j*, *open circles*), while the foci either uniquely labeled for TS28 (Fig. 4 *j*, *open triangles*) or labeled for both the α_1-DHPR and TS28 (Fig. 4 *j*, *crosses*) were generally confined to the cell periphery. The considerable variability in the number of foci in the three subclasses is most likely due to the fact that individual primary myotubes in 24-d fetal skeletal muscle are at somewhat different stages of development. However, a more extensive analysis will be required to determine if this is the case.

Newborn 1–2 d

α_1-DHPR versus TS28. Examination of transverse sections double labeled for the α_1-DHPR (Fig. 5, *a* and *c*) and for TS28 (Fig. 5, *b* and *d*) showed that all myofibers were positively labeled for both proteins. The α_1-DHPR was mostly confined to discrete foci present throughout the cytosol (Fig. 5, *a* and *c*). Occasionally, some foci appeared to be connected with faint fluorescent strands (Fig. 5, *a* and *c*). In contrast, TS28 was distributed in a chickenwire-like network present throughout the cytosol (Fig. 5, *b* and *d*). While the α_1-DHPR might codistribute with TS28 in parts of the TS28 positively labeled network, it appears that α_1-DHPR is not uniformly distributed in this network.

α_1-DHPR versus Ryanodine Receptor. Examination of transverse sections double labeled for the α_1-DHPR (Fig. 5, *e* and *g*) and for the ryanodine receptor (Fig. 5, *f* and *h*) showed that the labeling for the ryanodine receptor (Fig. 5, *f* and *h*) and the α_1-DHPR was confined to discrete foci present throughout the cytosol. Furthermore, the distribution of most of the foci positively labeled for the ryanodine receptor (e.g., Fig. 5 *h*, *arrowheads*) corresponded very closely to that of the foci positively labeled for the α_1-DHPR (Fig. 5 *g*, *arrowheads*). These results suggest that the ryanodine receptor and the α_1-DHPR also colocalize at this stage of development.

Ryanodine Receptor versus TS28. Examination of transverse sections at this stage of development double labeled for the ryanodine receptor (Fig. 5, *i* and *k*) and for TS28 (Fig. 5, *j* and *l*) confirmed the results described above. Thus, as shown in Fig. 5 *b*, TS28 was distributed in a chickenwire-like network present throughout the cytosol (Fig. 5, *j* and *l*). In contrast, the ryanodine receptor was mostly confined to discrete foci throughout the cytosol of all myofibers (Fig. 5, *i* and *k*).

Examination of longitudinal sections labeled for either the α_1-DHPR (Fig. 6, *a* and *b*), or for the ryanodine receptor (Fig. 6, *f* and *g*), showed that the distribution of labeling for the α_1-DPHR and the ryanodine receptor was confined to discrete foci present throughout the cytosol. Occasionally, these foci appeared to be aligned in rows oriented more or less parallel to the longitudinal axis of the myofiber (Fig. 6 *b*; α_1-DHPR; and Fig. 6 *g*; ryanodine receptor). In contrast, labeling for TS28 appeared as previously reported (45) to be distributed in an anastomosing network (Fig. 6, *c–e*). The longitudinally oriented component of the anastomosing network is more prominent than the transversely oriented component at this stage of development (Fig. 6, *d* and *e*).

Newborn 10 d and Adult

Examination of longitudinal cryosections from 10-d (Fig. 7,

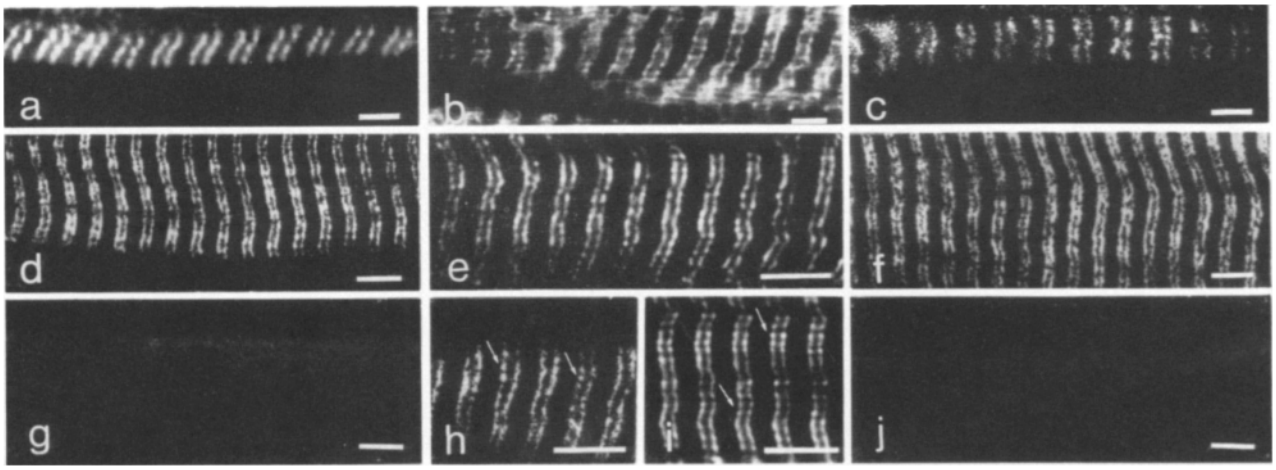

Figure 7. Localization of the α_1-DHPR, the ryanodine receptor, and TS28 in longitudinal cryosections of fixed 10-d and adult rabbit skeletal muscle by conventional immunofluorescence microscopy. Longitudinal cryosections of paraformaldehyde (2%) fixed 10-d-old (*a*, *b*, and *c*) and adult rabbit gracilis muscle (*d–j*) were labeled with affinity-purified antibodies to the α_1-DHPR (*a*, *d*, and *h*), with mAb IXE11$_2$ to TS28 (*b* and *e*), with affinity-purified antibodies to the ryanodine receptor (*c*, *f*, and *i*), with affinity-purified antibodies to the α_1-DHPR preadsorped with purified DHPR (*g*), and with affinity-purified antibodies to the ryanodine receptor preadsorped with purified ryanodine receptor (*j*). Specific labeling of 10-d-old (*a–c*) and adult skeletal muscle sections (*d–f*, *h* and *i*) for the α_1-DHPR (*a*, *d*, and *h*), TS28 (*b* and *e*) and ryanodine receptor (*c*, *f*, and *i*) appears as transversely oriented strands at the junction between the A- and I-bands as determined by phase-contrast microscopy (not shown). The specific fluorescence labeling for the α_1-DHPR seen in *d* and for the ryanodine receptor seen in *f* is greatly reduced after the preadsorption of these antibodies with purified DHPR (*g*) and ryanodine receptor (*j*), respectively. Arrows in *h* and *i* point to the position of A–I junctions in these fibers. Bars, 5 μm.

a–c) and adult gracilis muscle (Fig. 7, *d–j*) immunolabeled for the α_1-DHPR (Fig. 7, *a*, *d*, and *h*), TS28 (Fig. 7, *b* and *e*), and the ryanodine receptor (Fig. 7, *c*, *f*, and *i*), showed that at both stages of development the distribution of the specific labeling for all three antibodies was indistinguishable and generally confined to transversely oriented strands positioned at the A–I junction as determined by imaging the same field by phase-contrast microscopy (results not shown). The specific fluorescence labeling for the α_1-DHPR (Fig. 7 *h*, *arrows*) and for the ryanodine receptor (Fig. 7 *i*, *arrows*) sometimes appeared as a transversely oriented row of small bright foci at the A–I junctions in adult skeletal muscle fibers. When the antibodies to the α_1-DHPR and the ryanodine receptor were preadsorbed with highly purified DHPR and the ryanodine receptor, respectively, the specific labeling for the α_1-DHPR (Fig. 7 *d*) and for the ryanodine receptor (Fig. 7 *f*) was greatly reduced (Fig. 7, *g* and *j*, respectively).

Discussion

To assess at the cellular level whether the T-tubular proteins α_1-DHPR and TS28 are incorporated simultaneously or sequentially into forming T-tubules we have used double immunofluorescence labeling to compare the temporal appearance and subcellular distribution of TS28 to those of α_1-DHPR during the de novo biogenesis of T-tubules and triads in skeletal muscle developing in situ. On the basis of our previous immunofluorescence studies (45) we assume that the temporal appearance and subcellular distribution of TS28 represent those of forming T-tubules.

We conclude that in a particular developing myotube the α_1-DHPR appears before the onset of formation of T-tubules. This conclusion is supported by the results showing that positive labeling for TS28 was not detectable in some of the secondary myotubes in 19–24-d fetal muscle positively labeled for α_1-DHPR and is in agreement with results of previous studies on the ontogenesis of the DHPR in developing skeletal muscle (32, 36, 42) showing that a large increase in the number of nitrendipine binding sites (32, 36) and in the amount of mRNA of the α_1-DHPR (42) are concurrent with fusion of myoblasts into myotubes.

We also conclude that the subcellular distribution of α_1-DHPR and TS28 are generally distinct during the early stages of T-tubule formation. Thus, specific labeling for α_1-DHPR is distributed at the cell periphery and the outer zone of the cytosol of all myotubes while TS28 as previously shown (45) is confined to discrete foci at the cell periphery when it first appears. Subsequently, TS28 was in contrast to α_1-DHPR also present in rod-like structures projecting from the cell periphery towards the interior regions of the cytosol. Since α_1-DHPR is a membrane protein, these results are consistent with the idea that at early stages of myotube development the α_1-DHPR is first synthesized and incorporated into membrane-bound vesicles (Fig. 8; *AI*) that accumulate in the cytosol before the onset of T-tubule formation. This interpretation is also consistent with results presented by Romey et al. (32) showing that the level of DHPR ((+)-methyl-[^{3}H] PN 200–110 binding sites) in developing myotubes in culture reached its maximal level 2 d before the onset of T-tubule formation as assessed by EM and the appearance of spontaneous contractions. The subsequent presence of TS28, but not α_1-DHPR, in rod-like structures supports the idea that TS28 is fairly uniformly distributed in short tubular invaginations of the sarcolemma corresponding to forming T-tubules, while some α_1-DHPR–containing vesicles at the cell periphery become incorporated into discrete regions of forming T-tubules, and other α_1-DHPR–contain-

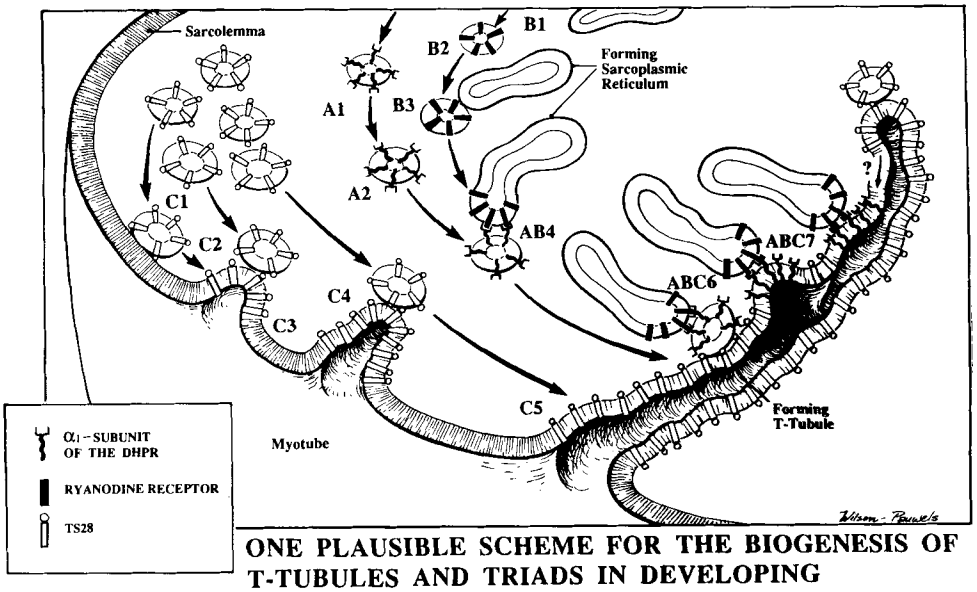

ONE PLAUSIBLE SCHEME FOR THE BIOGENESIS OF T-TUBULES AND TRIADS IN DEVELOPING SKELETAL MUSCLE

Figure 8. One plausible scheme for the biogenesis of T-tubules and triads in developing skeletal muscle. First, α_1-DHPR (*A1*) and ryanodine receptors (*B1*) are assumed to be synthesized on membrane-bound polyribosomes, incorporated into unique transfer vesicles, and distributed (*A2* and *B2*, respectively). Next, TS28-containing vesicles (*C1*) fuse first with the sarcolemma to form a caveolae (*C2*). Sequential fusions of TS28-containing vesicles to the caveolae result in the formation of a tubular invagination into the myotube (*C3–C5*). As this occurs, ryanodine receptor–containing vesicles are incorporated into forming SR (*B3*), followed by complex formation between ryanodine receptors in SR and the α_1-DHPR–containing transfer vesicles (*AB4*) in the outer zone of the cytosol. In turn, the α_1-DHPR–containing vesicle of this complex fuses with the TS28-containing forming T-tubules (*ABC6*), thus, incorporating the α_1-DHPR–containing vesicles into a discrete region of the forming T-tubules (*ABC7*) and forming a junctional complex between the T-tubule and the SR.

ing vesicles remain in the outer zone of the cytosol. This interpretation implies that α_1-DHPRs are not incorporated into forming T-tubules until after the biogenesis of TS28-containing T-tubules has begun.

This interpretation was further supported by analysis of tracings of confocal images of 24-d fetal muscle double labeled for TS28 and α_1-DHPR showing that ~50% (47 ± 15%) of the foci in primary myotubes were labeled for both the α_1-DHPR and TS28. Of the remaining foci, ~30% (31 ± 12%) were uniquely labeled for the α_1-DHPR, and ~20% (21 ± 10%) uniquely labeled for TS28. These results support the idea that only 60% of the α_1-DHPR–labeled foci are incorporated into T-tubules at this stage of development. The finding that most of the foci labeled for both TS28 and the α_1-DHPR are confined to the cell periphery and most of the foci uniquely labeled for the α_1-DHPR are in the outer zone of the cytosol is consistent with the idea that the α_1-DHPR at the cell periphery are incorporated into TS28 containing forming T-tubules (45) previously shown to be oriented parallel or obliquely to the long axis of the myotube (19, 34) at the cell periphery, and that the foci uniquely labeled for the α_1-DHPR represent α_1-DHPR–containing membrane vesicles in the outer zone of the cytosol where TS28–containing T-tubules are not yet present. The finding that most of the foci uniquely labeled for TS28 are confined to the cell periphery supports our previous proposal (45) that these foci may represent TS28-containing caveolae, or transverse and oblique sections of TS28-containing tubular structures at the cell periphery lacking the α_1-DHPR.

In myotubes from 1- to 2-d-old rabbit skeletal muscle, TS28, as previously shown (45), was distributed in a chicken-wire-like network in transverse sections and as an anastomosing network in longitudinal sections, suggesting that TS28 is uniformly distributed in both transverse and longitudinally oriented T-tubules. In contrast, most of the α_1-DHPR is distributed in discrete foci throughout the cytosol at this stage of development, indicating that α_1-DHPRs are incorporated into discrete regions of both longitudinally and transversely oriented T-tubules possibly corresponding to the region of the junctional complex between T-tubules and the forming junctional SR. This conclusion is consistent with the results of ultrastructural studies, showing that the junctional SR does not form a complete terminal cisternae along the T-tubules at this stage of development (34).

Assuming that the ryanodine receptor is a specific marker of the junctional region of the junctional SR (18), the temporal appearance of triads and T-tubules was assessed by comparing the subcellular distribution of the ryanodine receptor to that of TS28 and the α_1-DHPR in developing rabbit skeletal muscle. Generally, the results presented show that the temporal appearance and subcellular distribution of the ryanodine receptor are very similar to those of the α_1-DHPR but distinct from those of TS28. Thus, in primary and secondary myotubes from 19–24-d fetal rabbit skeletal muscle the ryanodine receptor is distributed in foci present in the outer zone of the cytosol supporting the possibility that the ryanodine receptor, like the α_1-DHPR, is a component of membrane-bound structures in this region of the cytosol (Fig. 8, *B1*). Since TS28 positive foci are generally absent from the outer zone of the cytosol of 19–24-d fetal myotubes, ryanodine receptor positive foci cannot be components of triads and are more likely components of membrane-bound vesicles either separate from or components of the forming SR. Since double labeling for the ryanodine receptor and the α_1-DHPR of 24-d fetal myotubes also showed that >80% of the foci positively labeled for the ryanodine receptor were also positively labeled for the α_1-DHPR, these results are consistent with the idea that most of the α_1-DHPR incorporated into the TS28-containing T-tubules forming at the cell periphery exist in a complex with ryanodine receptors pres-

ent either in discrete membrane vesicles (not shown) or in forming SR. Furthermore, these are also consistent with the idea that α_1-DHPR-positive but TS28-negative vesicles in the outer zone of the myotubes also form a complex with ryanodine receptors incorporated into either discrete vesicles (not shown) or into forming SR.

The results of double labeling the 1-2-d-old myotubes for the ryanodine receptor and the α_1-DHPR suggested that these two proteins colocalize in foci present in the cytosol. Comparison of these results with the results of double labeling for TS28 and the α_1-DHPR suggest that the α_1-DHPR incorporated into discrete regions of TS28-containing T-tubules also form a complex with ryanodine receptors incorporated into either discrete vesicles or into forming SR, thus, forming diad structures between T-tubules and either the junctional face of junctional SR or its precursor.

The sequence of events leading to the incorporation of TS28, the α_1-DHPR, and the ryanodine receptor into T-tubules and triads is presently unknown. However, on the basis of our previous studies of the assembly of TS28 into forming T-tubules (45), the results presented here, and current ideas about intracellular membrane trafficking, we propose the following plausible scheme for the correlation between the assembly of (*a*) TS28 and the α_1-DHPR into T-tubules; and (*b*) TS28, the α_1-DHPR, and the ryanodine receptor into a junctional complex between T-tubules and junctional SR (Fig. 8). First, α_1-DHPR (Fig. 8; *A1*) and ryanodine receptors (Fig. 8; *B1*) are synthesized on membrane-bound polyribosomes, incorporated into distinct vesicles, and distributed throughout the cytoplasm (Fig. 8, *A2* and *B2*, respectively). Next, TS28-containing vesicles fuse with the sarcolemma (Fig. 8, *C1*) thus forming caveolae (Fig. 8, *C2*). Sequential fusions of TS28-containing vesicles with forming T-tubules (Fig. 8, *C4*) result in the biogenesis of T-tubules (Fig. 8, *C5*). As the biogenesis of T-tubules occurs, ryanodine receptor-containing vesicles (Fig. 8, *B2*) are either (*a*) incorporated into forming SR (Fig. 8, *B3*) followed by formation of a complex between ryanodine receptors in the SR and a α_1-DHPR-containing vesicle (Fig. 8, *AB4*); or (*b*) form a complex with α_1-DHPR-containing vesicles in the interior region of the cytosol (not shown); in turn the α_1-DHPR-containing vesicle of this complex fuses with the TS28 containing forming T-tubules (Fig. 8, *ABC6*), thus incorporating the α_1-DHPR-containing vesicle of this complex into a discrete region of the forming T-tubules (Fig. 8, *ABC7*). Since the α_1-DHPR is complexed with the ryanodine receptor containing membrane system, incorporation of the α_1-DHPR into T-tubules also results in the formation of a junctional complex between T-tubules and the SR. It appears from the data presented that the α_1-DHPR does not become uniformly distributed along the forming T-tubules in rabbit skeletal muscle until 2 d after birth. However, the results presented do not permit us to conclude whether the α_1-DHPR becomes uniformly distributed throughout the T-tubules as development proceeds or remain confined within the junctional region of the T-tubules. Furthermore, these results do not permit us to conclude whether TS28 in the T-tubules becomes a component of the α_1-DHPR containing junctional region between T-tubules and junctional SR (diads and triads).

To assess the validity of the scheme proposed for the assembly of α_1-DHPR, TS28, and the ryanodine receptor into T-tubules and junctional complexes between T-tubules and junctional SR, it will be important to identify the subcellular organelles in developing muscle labeled with antibodies to these proteins by immunoelectron microscopy. These studies should also be helpful in delineating the intracellular pathway taken by the organelles transporting the α_1-DHPR, TS28, and the ryanodine receptor from the site of synthesis to the site of incorporation into their respective target membranes. This approach should furthermore determine whether the proposed interactions between the proposed "carrier" organelles indeed occur.

The scheme proposed for the assembly of T-tubules and triads implies that α_1-DHPR-containing vesicles play a pivotal role in the assembly of junctional complexes between forming T-tubules and ryanodine receptor containing junctional SR. In this regard, it is interesting that recent studies on dysgenic (mdg/mdg) muscle, an autosomal recessive mutation in mice characterized by the absence of excitation–contraction coupling (11) and a greatly decreased number of triads (30), have shown that the α_1-DHPR, but not the ryanodine receptor, is absent from the microsomal fraction of dysgenic muscle (22). Thus, developing dysgenic muscle should be an excellent model for testing at the cellular level the effect of lack of α_1-DHPR on the sequence of events leading to the biogenesis of T-tubules and triads including the effect on intracellular membrane pathways taking TS28 and the ryanodine receptor from the site of synthesis to their target organelles.

The generous gift of purified DHPR, purified ryanodine receptor and the corresponding antisera, as well as mAb IXE11$_2$ to TS28 from Dr. Kevin P. Campbell (Howard Hughes Medical Institute, Department of Physiology and Biophysics, University of Iowa, Iowa City) is very much appreciated. We gratefully acknowledge the artwork by Linda Wilson-Pawells, Acting Chairman of Art As Applied to Medicine, University of Toronto. The excellent technical assistance of Mr. Danny Hin-kie Ngai, Product Specialist at Biorad Laboratories (Canada) Limited in obtaining the immunofluorescence confocal images presented is gratefully acknowledged. We appreciate the generosity with which the Biorad Laboratories (Toronto, Canada) has made their Lasersharp MRC-500 confocal imaging system available to us.

Dr. Shaohua Yuan is a postdoctoral fellow of the Medical Research Council of Canada. Dr. Annelise O. Jorgensen is a Scientist of the Medical Research Council of Canada and recipient of Grant-in-aid MT 6364 from the Medical Research Council of Canada.

Received for publication 23 April 1990 and in revised form 24 September 1990.

References

1. Block, B. A., T. Imagawa, K. P. Campbell, and C. Franzini-Armstrong. 1988. Structural evidence for direct interaction between the molecular components of the transverse tubule/sarcoplasmic reticulum junction in skeletal muscle. *J. Cell Biol.* 107:2587–2600.
2. Brakenhoff, G. J., E. A. Van Spronsen, H. T. M. Van der Voort, and N. Nanninga. 1989. Three-dimensional confocal fluorescence microscopy. *In* Methods in Cell Biology. Vol. 30. D. L. Taylor and Y.-L. Wang, editors. Academic Press, New York. 379–398.
3. Campbell, K. P., and S. D. Kahl. 1989. Association of dystrophin and an integral membrane glycoprotein. *Nature (Lond.).* 338:259–262.
4. Campbell, K. P., A. T. Leung, and A. H. Sharp. 1988. The biochemistry and molecular biology of the dihydropyridine-sensitive calcium channel. *TINS Trends Neurosci.* 11:425–430.
5. Catterall, W. A., M. J. Seagar, and M. Takahashi. 1988. Molecular properties of dihydropyridine-sensitive calcium channels in skeletal muscle. *J. Biol. Chem.* 263:3535–3538.
6. Fleischer, S., and M. Inui. 1989. Biochemistry and biophysics of excitation-contraction coupling. *Annu. Rev. Biophys. Biophys. Chem.* 18:333–364.

7. Fosset, M., E. Jaimovich, E. Delpont, and M. Lazdunski. 1983. [^{3}H]Nitrendipine receptors in skeletal muscle: properties and preferential localization in transverse tubules. *J. Biol. Chem.* 258:6086–6092.
8. Fowler, V. M., and V. Bennett. 1984. Erythrocyte membrane tropomyosin: purification and properties. *J. Biol. Chem.* 259:5978–5989.
9. Franzini-Armstrong, C. 1973. Membranous systems in muscle fibers. *In* The Structure and Function of Muscle. Vol II. G. H. Bourne, editor. Academic Press, New York. 513–619.
10. Glossmann, H., and J. Striessnig. 1988. Structure and pharmacology of voltage-dependent calcium channels. *ISI Atlas Sci. Pharmacol.* 2:202–210.
11. Gluecksohn-Waelsch, S. 1963. Lethal genes and analysis of the differentiation. *Science (Wash. DC).* 142:1269–1276.
12. Imagawa, T., J. S. Smith, R. Coronado, and K. P. Campbell. 1987. Purified ryanodine receptor from skeletal muscle sarcoplasmic reticulum is the Ca^{2+}-permeable pore of the calcium release channel. *J. Biol. Chem.* 262:16636–16643.
13. Inui, M., A. Saito, and S. Fleischer. 1987. Purification of the ryanodine receptor and identity with feet structures of junctional terminal cisternae of sarcoplasmic reticulum from fast skeletal muscle. *J. Biol. Chem.* 262:1740–1747.
14. Johnson, D. A., J. W. Gautsch, J. R. Sportsman, and J. H. Elder. 1984. Improved technique utilizing nonfat dry milk for analysis of proteins and nucleic acids transferred to nitrocellulose. *Gene Anal. Tech.* 1:3–8.
15. Jorgensen, A. O., V. Kalnins, and D. H. MacLennan. 1979. Localization of sarcoplasmic reticulum proteins in rat skeletal muscle by immunofluorescence. *J. Cell Biol.* 80:372–384.
16. Jorgensen, A. O., A. C.-Y. Shen, W. Arnold, A. T. Leung, and K. P. Campbell. 1989. Subcellular distribution of the 1,4-dihydropyridine receptor in rabbit skeletal muscle in situ: an immunofluorescence and immunocolloidal gold-labeling study. *J. Cell Biol.* 109:135–147.
17. Jorgensen, A. O., W. Arnold, A. C.-Y. Shen, S. Yuan, M. Gaver, and K. P. Campbell. 1990. Identification of novel proteins unique to either transverse tubules (TS28) or the sarcolemma (SL50) in rabbit skeletal muscle. *J. Cell Biol.* 110:1173–1185.
18. Kawamoto, R. M., J.-P. Brunschwig, K. C. Kim, and A. H. Caswell. 1986. Isolation, characterization, and localization of the spanning protein from skeletal muscle triads. *J. Cell Biol.* 103:1405–1414.
19. Kelly, A. M. 1971. Sarcoplasmic reticulum and T tubules in differentiating rat skeletal muscle. *J. Cell Biol.* 49:335–344.
20. Kelly, A. M., and S. I. Zacks. 1969. The histogenesis of rat intercostal muscle. *J. Cell Biol.* 42:135–153.
21. Kilarski, W., and M. Jakubowska. 1979. An electron microscopy study of the myofibril formation in embryonic rabbit skeletal muscle. *Z. Mikrosk. Anat. Forsch. (Leipz.).* 93:1159–1181.
22. Knudson, C. M., N. Chaudhari, A. H. Sharp, J. A. Powell, K. G. Beam, and K. P. Campbell. 1989. Specific absence of the α_1 subunit of the dihydropyridine receptor in mice with muscular dysgenesis. *J. Biol. Chem.* 264:1345–1348.
23. Knudson, C. M., J. R. Mickelson, C. F. Louis, and K. P. Campbell. 1990. Distinct immunopeptide maps of the sarcoplasmic reticulum Ca^{2+} release channel in malignant hyperthermia. *J. Biol. Chem.* 265:2421–2424.
24. Laemmli, U. K. 1970. Cleavage of structural proteins during the assembly of the head of bacteriophage T4. *Nature (Lond.).* 227:680–685.
25. Lai, F. A., H. P. Erickson, E. Rousseau, Q.-Y. Liu, and G. Meissner. 1988. Purification and reconstitution of the calcium release channel from skeletal muscle. *Nature (Lond.).* 331:315–319.
26. Leung, A., T. Imagawa, B. Block, C. Franzini-Armstrong, and K. P. Campbell. 1988. Biochemical and ultrastructural characterization of the 1,4-dihydropyridine receptor from rabbit skeletal muscle: evidence for a 52,000 Da subunit. *J. Biol. Chem.* 263:994–1001.
27. Lowry, O. H., N. J. Rosebrough, A. L. Farr, and R. J. Randall. 1951. Protein measurement with the folin phenol reagent. *J. Biol. Chem.* 193: 265–275.
28. McLennan, I. S. 1983. Differentiation of muscle fiber types in the chicken hindlimb. *Dev. Biol.* 97:222–228.
29. Peterson, G. L. 1977. A simplification of the protein assay method of Lowry et al. which is more generally applicable. *Anal. Biochem.* 83: 346–356.
30. Pincon-Raymond, M., F. Rieger, M. Fosset, and M. Lazdunski. 1985. Abnormal transverse tubule system and abnormal amount of receptors for Ca^{2+} channel inhibitors of the dihydropyridine family in skeletal muscle from mice with embryonic muscular dysgenesis. *Dev. Biol.* 112:458–466.
31. Rios, E., and G. Brum. 1987. Involvement of dihydropyridine receptors in excitation–contraction coupling in skeletal muscle. *Nature (Lond.).* 325:717–720.
32. Romey, G., L. Garcia, V. Dimitriadou, M. Pincon-Raymond, F. Rieger, and M. Lazdunski. 1989. Ontogenesis and localization of Ca^{2+} channels in mammalian skeletal muscle in culture and role in excitation-contraction coupling. *Proc. Natl. Acad. Sci. USA.* 86:2933–2937.
33. Saito, A., M. Inui, M. Radermacher, J. Frank, and S. Fleischer. 1988. Ultrastructure of the calcium release channel of sarcoplasmic reticulum. *J. Cell Biol.* 107:211–219.
34. Schiaffino, S., and A. Margreth. 1969. Coordinated development of the sarcoplasmic reticulum and T system during postnatal differentiation of rat skeletal muscle. *J. Cell Biol.* 41:855–875.
35. Schiaffino, S., M. Cantini, and S. Sartore. 1977. T-system formation in cultured rat skeletal tissue. *Tissue & Cell.* 9:437–446.
36. Schmid, A., J.-F. Renaud, M. Fosset, J.-P. Meaux, and M. Lazdunski. 1984. The nitrendipine-sensitive Ca^{2+} channel in chick muscle cells and its appearance during myogenesis in vitro and in vivo. *J. Biol. Chem.* 259:11366–11372.
37. Smith, J. S., T. Imagawa, K. P. Campbell, and R. Coronado. 1988. Purified ryanodine receptor from rabbit skeletal muscle is the calcium release channel of sarcoplasmic reticulum. *J. Gen. Physiol.* 92:1–26.
38. Tanabe, T., H. Takeshima, A. Mikami, V. Flockerzi, H. Takahashi, K. Kangawa, M. Kojima, H. Matsuo, T. Hirose, and S. Numa. 1987. Primary structure of the receptor for calcium channel blockers from skeletal muscle. *Nature (Lond.).* 328:313–318.
39. Tanabe, T., K. G. Beam, J. A. Powell, and S. Numa. 1988. Restoration of excitation-contraction coupling and slow calcium current in dysgenic muscle by dihydropyridine receptor complementary DNA. *Nature (Lond.).* 336:134–139.
40. Towbin, H., T. Staehelin, and J. Gordon. 1979. Electrophoretic transfer of proteins from polyacrylamide gels to nitrocellulose sheets: procedure and some applications. *Proc. Natl. Acad. Sci. USA.* 76:4350–4354.
41. Tung, A. S. 1983. Production of large amounts of antibodies, nonspecific immunoglobulins, and other serum proteins in ascitic fluids of individual mice and guinea pigs. *Methods Enzymol.* 93:12–23.
42. Varadi, G., J. Orlowski, and A. Schwartz. 1989. Developmental regulation of expression of the α_1 and α_2 subunits mRNAs of the voltage-dependent calcium channel in a differentiating myogenic cell line. *FEBS (Fed. Eur. Biochem. Soc.) Lett.* 250:515–518.
43. Wagenknecht, T., R. Grassucci, J. Frank, A. Saito, M. Inui, and S. Fleischer. 1989. Three-dimensional architecture of the calcium channel/foot structure of sarcoplasmic reticulum. *Nature (Lond.).* 338:167–170.
44. White, J. G., W. B. Amos, and M. Fordham. 1987. An evaluation of confocal versus conventional imaging of biological structures by fluorescence light microscopy. *J. Cell Biol.* 105:41–48.
45. Yuan, S., W. Arnold, and A. O. Jorgensen. 1990. Biogenesis of transverse tubules: immunocytochemical localization of a transverse tubular protein (TS28) and sarcolemmal protein (SL50) in rabbit skeletal muscle developing in situ. *J. Cell Biol.* 110:1187–1198.